

## On the Dynamic Regulation of Three-Layer Stratified Flow through Porous Media

Sameh A. Alkharashi<sup>1,2,\*</sup>, Khaled Al-Hamad<sup>1</sup> and Azizah Alrashidi<sup>1</sup>

<sup>1</sup> Applied Sciences Department, College of Technological Studies, PAAET, Kuwait

<sup>2</sup> Quesna Technical College, Ministry of Higher Education, Cairo, Egypt

\* Corresponding author

Copyright © 2018 Sameh A. Alkharashi, Khaled Al-Hamad and Azizah Alrashidi. This article is distributed under the Creative Commons Attribution License, which permits unrestricted use, distribution, and reproduction in any medium, provided the original work is properly cited.

### Abstract

Stability properties of two-dimensional viscous fluid layers moving in porous media is examined. The system is composed of a middle fluid embedded between two semi-infinite fluids, in which the effect of the electric field is to introduce. The principle aim of this work is to investigate the influence of fluid viscosity and the porosity effect on the growth rate in the presence of horizontal electric field. The parameters governing the layers flow system, the electric properties and porosity effects strongly influence the wave forms and their amplitudes and hence the stability of the fluid. The stability criteria are performed theoretically in which stability diagrams are obtained. It is established that the phenomenon of the dual role is found for increasing the permeability parameter as well as the dielectric ratio. It has been found that both the viscosity coefficient and the electric field damps the growth rate, introducing stabilizing influence. The role of Reynolds number and the density ratio is to increase the amplitude of the disturbance leading to the destabilization state of the flow system, promote the oscillatory

behavior. Influence of the various parameters of the problem on the interface stability is thoroughly analyzed.

**Keywords:** Electric Field; Viscous Fluids; Three Layers Stability; Porous Media.

## 1 Introduction

Behavior of moving layers under certain conditions has fascinated many researchers due to their conceptual simplicity, rich dynamical phenomenology and technological relevance and has attracted considerable interest since the pioneering theoretical and experimental investigations.

Previous researches have shown the importance of studying the hydrodynamic stability problems, for example the influence of viscosity on the stability of the plane interface separating two incompressible superposed fluids of uniform densities, when the whole system is immersed in a uniform horizontal magnetic field, has been studied in the paper [1]. In the research [2] the authors have carried out the instability of viscous potential flow in a horizontal rectangular channel. The analysis leads to an explicit dispersion relation in which the effects of surface tension and viscosity on the normal stress are not neglected but the effect of shear stresses is. The unsteady electrohydrodynamic stability has been investigated by Elhefnawy [3], where the stability analysis has been made of a basic flow of streaming fluids in the presence of an oblique periodic electric field. A series of studies for hydrodynamics stability have also been initiated by Drazin and Reid [4] and Joseph [5].

The authors in paper [6] have investigated the stability properties of time periodically streaming superposed magnetic fluids through porous media under the influence of an oblique alternating magnetic field, where the system is composed of a middle fluid sheet of finite thickness embedded between two other bounded layers. Also, Zakaria *et al.* [7] have analyzed the effect of an externally applied electric field on the stability of a thin fluid film over an inclined porous plane, using linear and non-linear stability analysis in the long wave limit. They found that the permeability parameter, as well as the inclination of the plane, play a destabilizing role in the stability criteria, while the damping influence is observed for increasing of the electrical conductivity in both linear and non-linear behavior.

Wray *et al.* [8] have investigated the evolution and stability of a wetting viscous fluid layer flowing down the surface of a cylinder, and surrounded by

a conductive gas. Liu *et al.* [9] have studied the instability properties of two-dimensional non-Newtonian liquid sheets moving in an inviscid gaseous environment. They found that non-Newtonian liquid sheets have a higher growth rate than Newtonian liquid sheets for both symmetric and antisymmetric disturbances, indicating that non-Newtonian liquid sheets are more unstable than Newtonian liquid sheets.

Based on a modified Darcy's law for a viscoelastic fluid, Sirwah [10] has discussed the linear stability analysis of the electrified surface separating two coaxial Oldroyd-B fluid layers confined between two impermeable rigid cylinders in the presence of both interfacial insoluble surfactant and surface charge through porous media. Also, Tan and Masuoka [11] have extended Stokes first problem to that for an Oldroyd-B fluid in a porous half space, where an exact solution was obtained by using Fourier sine transform. Zakaria [12] has investigated the time evolution of superposed layers of fluid flowing down inside an inclined permeable channel. Using the Kármán-Pohlhausen approximation, the problem is reduced to the study of the evolution equation for the liquid-liquid interface of the liquids film derived through a long wave approximation. In this research the solutions and stability of the non-linear stationary long waves are investigated. Khan *et al.* [13] have demonstrated the analytical solutions for the magnetohydrodynamic flow of an Oldroyd-B fluid through a porous medium. They obtained the expressions for the velocity field and the tangential stress by means of the Fourier sine transform. Kumar and Singh [14] have investigated the stability of a plane interface separating two viscoelastic (Rivlin-Ericksen) superposed fluids in the presence of suspended particles. They concluded that the system is stable for stable configuration and unstable for unstable configuration in the presence of suspended particles.

In this article, the considered system is composed of a viscous fluid layer of finite thickness embedded between two semi-infinite fluids. The system is influenced by horizontal electric field. The objective of the present work is to investigate the mechanisms of stability of three porous layers of fluids in the presence of horizontal electric field. The plan of this work is as follows: This section has presented the motivation for the investigation in addition to relevant background information. In next section, we will give a description of flow configuration and the stability statement including the basic equations of the fluid mechanics and Maxwell's equations governing the motion of our model. In the third section and its subsections, are concerned with the derivation of the characteristic equation and numerical applications for stability configuration. The salient results of our analysis are discussed and some important

conclusions are drawn in the final section of this paper.

## 2 Flow configuration and the stability statement

### 2.1 Mathematical model

A two-dimensional system of an infinite horizontal viscous fluid sheet of vertical height  $2d$  confined between two semi-infinite superposed incompressible viscous fluids is considered. The  $x$ -axis of the coordinate system is parallel to the direction of the fluid sheet flow, and the  $y$ -axis is normal to the fluid sheet with its origin located at the middle plane of the fluid sheet as shown in Fig. 1.

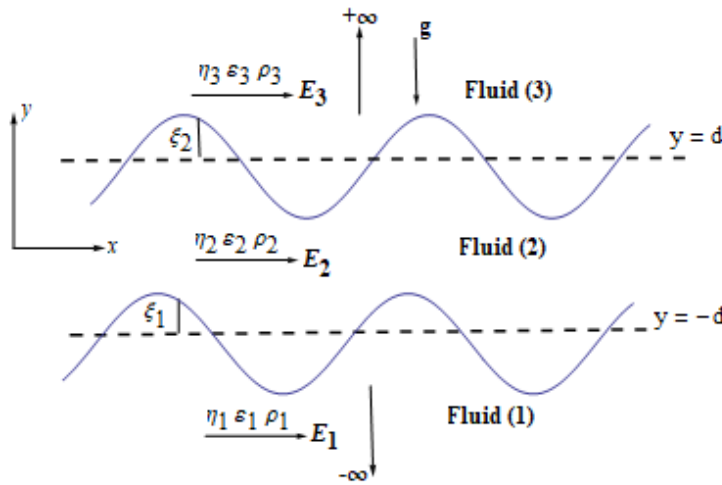


Figure 1: Schematic representation of problem geometry.

The lower fluid occupies the region  $-\infty < y < -d$ , the middle fluid is contained in the region typified by  $-d < y < d$  while the range  $d < y < \infty$  represents the upper fluid. The system is considered to be influenced by the gravity force  $\mathbf{g}(0, g)$  in the negative  $y$ -direction. The two interfaces between the fluids are assumed to be well defined and initially flat and form the interfaces  $y = -d$  and  $y = d$ . The two interfaces are parallel and the flow in each phase is everywhere parallel to each other. The surface deflections are expressed by  $y = \xi_1(x, t)$  at  $y = -d$  and  $y = \xi_2(x, t)$  at  $y = d$ , where  $y = \pm d$  are the equilibrium positions of the two interfaces, i.e. the positions without disturbances,  $\xi_l$ , ( $l = 1, 2$ ) is the size of the disturbance at a point.

In the following, we will use the dimensionless variables to provide improved insight into the physics and in order to understand hydrodynamic stability better. So we define the corresponding dimensionless variables using the half thickness of the middle fluid sheet  $d$  as a length scale. Thus the stream velocity and the time are made dimensionless using  $\sqrt{dg}$  and  $\sqrt{d/g}$ , while the applied electric field and the electric potential are made dimensionless by  $\sqrt{dg\rho_2/\varepsilon_2}$  and  $d\sqrt{dg\rho_2/\varepsilon_2}$ , respectively. In addition the viscosity  $\rho_2\sqrt{d^2g}$ , the pressure  $dg\rho_2$ , the stream function  $\sqrt{d^3g}$  and the permeability of the porous medium  $d^2Q$ . Furthermore, in the equations of motion, we use the symbols: the dielectric constant ratio  $\hat{\varepsilon}_j = \varepsilon_j/\varepsilon_2$  the fluid density ratio  $\hat{\rho}_j = \rho_j/\rho_2$  the dynamic viscosities ratio  $\hat{\eta}_j = \eta_j/\eta_2$  ( $j = 1, 2, 3$ ). Also the Weber number  $W_l = T_l/d^2g\rho_2$ , ( $l = 1, 2$ ), where  $T_l$  is the surface tension coefficient.

## 2.2 Governing equations and boundary conditions

Assuming a quiescent initial state, therefore the base state velocity in the fluid layers is zero in which the flow is steady and fully developed. Thus the fundamental nondimensional equations governing the motion of the electric fluids are coming out from the ordinary hydrodynamic equations and Maxwell's relations of electric field [2-6].

$$\hat{\rho}_j R_e D_t u_j = -R_e \partial_x \Pi_j + \hat{\eta}_j (\nabla^2 u_j + \frac{u_j}{Q_j}), \quad j = 1, 2, 3, \quad (1)$$

$$\hat{\rho}_j R_e D_t v_j = -R_e \partial_y \Pi_j + \hat{\eta}_j (\nabla^2 v_j + \frac{v_j}{Q_j}), \quad (2)$$

associated with the continuity equation which expresses the conservation of mass:

$$\partial_x u_j + \partial_y v_j = 0, \quad (3)$$

where  $R_e = \rho_2\sqrt{d^3g}/\eta_2$  denotes the Reynolds number of the middle layer and  $Q_j$  represents the permeability parameter and  $\Pi_j = p_j + \rho_jgy$  is the total hydrostatic pressure. In addition  $D_t \equiv \partial_t + (\mathbf{u} \cdot \nabla)$  stands for the convective derivative,  $\partial_t$  is the partial derivative with respect to the time  $t$ ,  $\nabla \equiv (\partial_x, \partial_y)$  is the horizontal gradient operator.

In formulating Maxwell's equations for the problem, we supposed that the electro-quasi-static approximation is valid for the problem, i.e. the effects of the magnetic fields due to the slow variations in the electric fields are negligible. This assumption requires the electric field to be both curl and divergence free and consequently we have

$$\nabla \cdot (\varepsilon_j \mathbf{E}_j) = 0 \quad \text{and} \quad \nabla \times \mathbf{E}_j = \mathbf{0}. \quad (4)$$

Here,  $\mathbf{E}_j$  is the electric field intensity vector, the notation  $\times$  refers to the vector product of two vectors and  $\varepsilon_j$  refers to the dielectric constant. The construction of a potential function  $\varphi_j$ , can be representable as the gradient of the scalar potential such that

$$\mathbf{E}_j = (E_{0j} - \partial_x \varphi_j) \mathbf{e}_x - \partial_y \varphi_j \mathbf{e}_y, \quad (5)$$

automatically satisfies zero curl for a constant permittivity and therefore the electrostatic potential satisfies the Laplace equation

$$\partial_x^2 \varphi_j + \partial_y^2 \varphi_j = 0, \quad (6)$$

where  $\mathbf{e}_x$  and  $\mathbf{e}_y$  are unit vectors in  $x$ - and  $y$ - directions. The Maxwell stress tensor describes the stress field induced in the material due to electrostatic forces whose expression is

$$\mathbf{M}_j = \varepsilon_j \left( \mathbf{E}_j \mathbf{E}_j - \frac{1}{2} (\mathbf{E}_j \cdot \mathbf{E}_j) \mathbf{I} \right), \quad (7)$$

where,  $\mathbf{I}$  is the identity tensor. It is to be noted here that the divergence of the Maxwell stress tensor in the bulk fluid is zero because the bulk of the fluid is free of net charge, and the dielectric constants are independent of spatial position in the fluid. Thus, the Maxwell stress tensor not appear in the momentum equation above, but will affect the flow only through the conditions at the interface.

In order to complete the formulation of the problem, the boundary conditions have to be specified. Since at the boundaries among fluids, the fluids and the electric stresses must be balanced. The components of these stresses consist of the hydrodynamics pressure, surface tension, porosity effects and electric stresses [15, 16]. The boundary conditions represented here are prescribed at the interface  $y = \xi_l(x, t)$ , where  $\xi_l$  is the height of the disturbed interfaces away from its initial position ( $y = \pm 1$ ) which is defined in the next section. As the interface is deformed all variables are slightly perturbed from their equilibrium values. Because the interfacial displacement is small, the boundary conditions on perturbation interfacial variables need to be evaluated at the equilibrium position rather than at the interface. Therefore, it is necessary to express all the physical quantities involved in terms of Taylor series about  $y = \pm 1$ .

The flow field solutions of the above governing equations have to satisfy the kinematic and dynamic boundary conditions at the two interfaces, which can be taken as  $y \approx \pm 1$  (the first order approximation for a small displacement of the interfaces due to the disturbance). The normal component of the velocity

vector in each of the phases of the system is continuous at the dividing surface. This implies that

$$\mathbf{n}_l \cdot (\mathbf{u}_l - \mathbf{u}_{l+1}) = 0, \quad y = (-1)^l, \quad l = 1, 2, \quad (8)$$

where  $\mathbf{n}_l$  is the outward normal unit vector to the interfaces which are given from the relation,  $\mathbf{n}_l = \nabla S_l / |\nabla S_l|$  and  $S_l(x, y, t)$  is the surface geometry defined by  $S_l = y - \xi_l(x, t) = \pm 1$ .

The condition that the interfaces are moving with the fluids ( $D_t S_l = 0$ ) lead to

$$v_{l,(l+1)} + \partial_t \xi_l = 0, \quad y = (-1)^l, \quad l = 1, 2. \quad (9)$$

In addition the jump in the shearing stresses is zero across the interfaces, this gives

$$|[\hat{\eta}_l (\partial_y u_l + \partial_x v_l)]|_l^{l+1} = 0, \quad y = (-1)^l, \quad l = 1, 2, \quad (10)$$

where, the notation  $[[X]]$  is used here to signify the difference in some quantity  $X$  across the interfaces.

Furthermore, Maxwell's conditions on the electric field where no free surface charges are present on the interfaces. The continuity of the normal component of the electric displacement at the interfaces reads:

$$\mathbf{n}_l \cdot (\hat{\epsilon}_l \mathbf{E}_l - \mathbf{E}_{l+1}) = 0, \quad y = (-1)^l, \quad l = 1, 2, \quad (11)$$

which gives

$$\begin{aligned} \partial_y \varphi_2 - \hat{\epsilon}_1 \partial_y \varphi_1 &= (\hat{\epsilon}_1 - 1) E_{01} \partial_x \xi_1, & y = -1, \\ \partial_y \varphi_2 - \hat{\epsilon}_3 \partial_y \varphi_3 &= (\hat{\epsilon}_3 - 1) E_{01} \partial_x \xi_2, & y = 1. \end{aligned}$$

The tangential component of the electric field is zero across the interfaces, this requires that

$$\mathbf{n}_l \times (\mathbf{E}_l - \mathbf{E}_{l+1}) = 0, \quad y = (-1)^l, \quad l = 1, 2, \quad (12)$$

from this equation, we have

$$\partial_x \varphi_2 - \partial_x \varphi_1 = 0 \quad \text{at} \quad y = -1 \quad \text{and} \quad \partial_x \varphi_3 - \partial_x \varphi_2 = 0 \quad \text{at} \quad y = 1.$$

The completion of the mathematical description of the problem requires an additional interfacial condition determine the shape of the interface between the fluids, which is the dynamical equilibrium boundary condition in which the surface traction suffers a discontinuity due to the surface tension:

$$|[\mathbf{n}_l \cdot \boldsymbol{\tau} \cdot \mathbf{n}_l]|_l^{l+1} = W_l \nabla \cdot \mathbf{n}_l, \quad y = (-1)^l, \quad l = 1, 2. \quad (13)$$

The stress tensor,  $\tau$ , is composed of a fluid component (isotropic pressure and deviatoric viscous stresses for the Newtonian fluid),  $\tau^{(f)}$ , and an electrical component,  $\tau^{(e)}$ , whose expressions are given by the formulas

$$\tau_l^{(f)} = -p_l \mathbf{I} + \hat{\eta}_l (\nabla \mathbf{u}_l + \nabla \mathbf{u}_l^{T_r}), \quad (14)$$

$$\tau_l^{(e)} = \hat{\varepsilon}_l \left( \mathbf{E}_l \mathbf{E}_l - \frac{1}{2} (\mathbf{E}_l \cdot \mathbf{E}_l) \mathbf{I} \right), \quad (15)$$

where the symbol  $\mathbf{I}$  denotes the identity tensor, while the superscript  $T_r$  indicates the matrix transpose. Thus the dynamical condition becomes

$$\left[ -p + 2\hat{\eta} \frac{\partial v}{\partial y} + \hat{\varepsilon} (E_n^2 - \frac{1}{2} E^2) \right] \Big|_l^{l+1} = W_l \nabla \cdot \mathbf{n}_l. \quad (16)$$

### 2.3 Linear perturbation

In order to investigate the stabilization of the present problem, the interfaces between the fluids will be assumed to be perturbed about its equilibrium location and will cause a displacement of the material particles of the fluid system. This displacement may be described by the equation

$$\xi_l(x, t) = \hat{\xi}_l e^{ikx + \omega t} + c.c., \quad l = 1, 2, \quad (17)$$

where  $\hat{\xi}_l$  is the initial amplitude of the disturbance, which is taken to be much smaller than the half-thickness  $d$  of the middle sheet,  $k$  is the wave number of the disturbance, which is assumed to be real and positive ( $k = 2\pi/\lambda$ , where  $\lambda$  is the wavelength of the disturbance),  $\omega$  is a complex frequency ( $\omega = \omega_r + i\omega_i$ , where  $\omega_r$  represents the rate of growth of the disturbance,  $\omega_i$  is  $2\pi$  times the disturbance frequency), the symbol  $i$  denotes  $\sqrt{-1}$ , the imaginary number and  $c.c$  represents the complex conjugate of the preceding terms.

The equations of motion and the boundary conditions mentioned previously will be solved under the assumption that the perturbations are small, so, all equations of motion and boundary conditions will be linearized in the perturbed quantities.

The solution of the above system of governing equations and boundary conditions can be facilitated by defining a stream function,  $\psi$  of the time and space coordinates, which automatically satisfies Eq. (3), where

$$u = \partial_y \psi, \quad v = -\partial_x \psi. \quad (18)$$

Using the normal mode approach we write the perturbations in the form

$$\psi = \hat{\psi}(y) e^{ikx + \omega t} + c.c. \quad (19)$$

Eliminating the pressure term from Eqs. (1) and (2) and using (18) and (19), we obtain the following equation

$$D_y^4 \hat{\psi}_j - (\ell_j^2 + k^2) D_y^2 \hat{\psi}_j + k^2 \ell_j^2 \hat{\psi}_j = 0, \quad (20)$$

where  $D_y = d/dy$  and

$$\ell_j = \sqrt{k^2 + \frac{\hat{\rho}_j R_e \omega}{\hat{\eta}_j} + \frac{1}{Q_j}}.$$

It is obvious that the analytical solution of Eq. (20) is of the form

$$\hat{\psi}_j(y) = A_{1j} e^{ky} + A_{2j} e^{-ky} + A_{3j} e^{\ell_j y} + A_{4j} e^{-\ell_j y}. \quad (21)$$

Since the boundary conditions require that the disturbances vanish as  $y \rightarrow \pm\infty$  (i.e.  $A_{21} = A_{41} = A_{13} = A_{33} = 0$ ). Thus we have the stream function in the three layers:

$$\begin{aligned} \psi_1 &= (A_{11} e^{ky} + A_{31} e^{\ell_1 y}) e^{ikx+\omega t} + c.c., \quad y < -1, \\ \psi_2 &= (A_{12} e^{ky} + A_{22} e^{-ky} + A_{32} e^{\ell_2 y} + A_{42} e^{-\ell_2 y}) e^{ikx+\omega t} + c.c., \quad -1 < y < 1, \\ \psi_3 &= (A_{23} e^{-ky} + A_{43} e^{-\ell_3 y}) e^{ikx+\omega t} + c.c., \quad y > 1. \end{aligned} \quad (22)$$

Using the normal mode solution we can obtain the pressure from Eqs. (1) and (2):

$$p_j = \frac{1}{ik} \left\{ \frac{\hat{\eta}_j}{R_e} \left[ \partial_y^3 \psi_j + \partial_x^2 \partial_y \psi_j - Q_j^{-1} \partial_y \psi_j \right] - \hat{\rho}_j \partial_x \partial_t \psi_j \right\}. \quad (23)$$

The solution of the electric potential, in view of Eqs.(6) may be taken the form

$$\begin{aligned} \varphi_1 &= B_{11} e^{ikx+ky+\omega t} + c.c., \quad y < -1, \\ \varphi_2 &= (B_{12} e^{ky} + B_{22} e^{-ky}) e^{ikx+\omega t} + c.c., \quad -1 < y < 1, \\ \varphi_3 &= B_{23} e^{ikx-ky+\omega t} + c.c., \quad y > 1. \end{aligned} \quad (24)$$

## 3 Results and discussion

### 3.1 Derivation of the characteristic equation

In this section, we will derive the dispersion relation controlling the stability behavior of the system. When the obtained solutions of the stream function,

electric potential and surface tension are inserted into Eqs. (8-16), we have a linear homogeneous system of algebraic equations of the fourteen unknown coefficients  $A_{pj}$ ,  $B_{lj}$ ,  $\hat{\xi}_l$ , ( $p = 1, 2, 3, 4$ ). This homogeneous system of equations can be expressed in matrix form as

$$\mathbf{AX} = \mathbf{0}, \quad (25)$$

where  $\mathbf{0}$  is a null vector,  $\mathbf{X}$  is a vector of unknown coefficients defined as

$$\mathbf{X}^{Tr} = \left( A_{11}, A_{31}, A_{12}, A_{22}, A_{32}, A_{42}, A_{23}, A_{43}, B_{11}, B_{12}, B_{22}, B_{23}, \hat{\xi}_1, \hat{\xi}_2 \right), \quad (26)$$

and the coefficient matrix  $\mathbf{A}$  is given by

$$\begin{pmatrix} ike^{-k} & ike^{-\ell_1} & 0 & 0 & 0 & 0 & 0 & 0 \\ 0 & 0 & ike^{-k} & ike^k & ike^{-\ell_2} & ike^{\ell_2} & 0 & 0 \\ 0 & 0 & ike^k & ike^{-k} & ike^{\ell_2} & ike^{-\ell_2} & 0 & 0 \\ 0 & 0 & 0 & 0 & 0 & 0 & ike^{-k} & 0 \\ 2\hat{\eta}_1 k^2 e^{-k} & \hat{\eta}_1 (k^2 + \ell_1^2) e^{-\ell_1} & -2k^2 e^{-k} & -2k^2 e^k & -(k^2 + \ell_2^2) e^{-\ell_2} & -(k^2 + \ell_2^2) e^{\ell_2} & 0 & 0 \\ 0 & 0 & 2k^2 e^k & 2k^2 e^{-k} & (k^2 + \ell_2^2) e^{\ell_2} & (k^2 + \ell_2^2) e^{-\ell_2} & -2\hat{\eta}_3 k^2 e^{-k} & 0 \\ ke^{-k} & \ell_1 e^{-\ell_1} & -ke^{-k} & ke^k & -\ell_2 e^{-\ell_2} & \ell_2 e^{\ell_2} & 0 & 0 \\ 0 & 0 & ke^k & -ke^{-k} & \ell_2 e^{\ell_2} & -\ell_2 e^{-\ell_2} & ke^{-k} & 0 \\ 0 & 0 & 0 & 0 & 0 & 0 & 0 & 0 \\ 0 & 0 & 0 & 0 & 0 & 0 & 0 & 0 \\ 0 & 0 & 0 & 0 & 0 & 0 & 0 & 0 \\ 0 & 0 & 0 & 0 & 0 & 0 & 0 & 0 \\ \hat{A}_{11} & 2ik\ell_1 \hat{\eta}_1 e^{-\ell_1} & \hat{A}_{12} & \hat{A}_{22} & -2ik\ell_2 e^{-\ell_2} & 2ik\ell_2 e^{\ell_2} & 0 & 0 \\ 0 & 0 & \hat{A}_{12} & \hat{A}_{22} & 2ik\ell_2 e^{\ell_2} & -2ik\ell_2 e^{-\ell_2} & \hat{A}_{23} & 0 \\ \\ 0 & 0 & 0 & 0 & 0 & 0 & \omega & 0 \\ 0 & 0 & 0 & 0 & 0 & 0 & \omega & 0 \\ 0 & 0 & 0 & 0 & 0 & 0 & 0 & \omega \\ ike^{-\ell_3} & 0 & 0 & 0 & 0 & 0 & 0 & \omega \\ 0 & 0 & 0 & 0 & 0 & 0 & 0 & 0 \\ -\hat{\eta}_3 (k^2 + \ell_3^2) e^{-\ell_3} & 0 & 0 & 0 & 0 & 0 & 0 & 0 \\ 0 & 0 & 0 & 0 & 0 & 0 & 0 & 0 \\ -\ell_3 e^{-\ell_3} & 0 & 0 & 0 & 0 & 0 & 0 & 0 \\ 0 & k\hat{\varepsilon}_1 e^{-k} & -ke^{-k} & ke^k & 0 & ik(\hat{\varepsilon}_1 - 1)E_{01} & 0 & 0 \\ 0 & 0 & ke^k & -ke^{-k} & k\hat{\varepsilon}_3 e^{-k} & 0 & ik(\hat{\varepsilon}_3 - 1)E_{01} & 0 \\ 0 & -ike^{-k} & ike^{-k} & ike^k & 0 & 0 & 0 & 0 \\ 0 & 0 & -ike^k & -ike^{-k} & ike^{-k} & 0 & 0 & 0 \\ 0 & -ik\hat{\varepsilon}_1 E_{01} e^{-k} & ikE_{01} e^{-k} & ikE_{01} e^k & 0 & \hat{\xi}_1 & 0 & 0 \\ 2ik\ell_3 \hat{\eta}_3 e^{-\ell_3} & 0 & -ikE_{01} e^k & -ikE_{01} e^{-k} & ik\hat{\varepsilon}_3 E_{01} e^{-k} & 0 & 0 & \hat{\xi}_2 \end{pmatrix} \quad (27)$$

where

$$\hat{A}_{11} = Q_1^{-1} e^{-k} \{ Q_1 (2i\hat{\eta}_1 k^2 - \hat{\rho}_1 \omega) - 1 \}, \hat{A}_{12} = Q_2^{-1} e^{(-1)^l k} \{ Q_2 (\omega + 2(-1)^l ik^2) + 1 \}, \\ l = 1, 2,$$

$$\check{A}_{12} = e^{-k}(2ik^2 - \omega - Q_2^{-1}), \quad \check{A}_{22} = -Q_2^{-1}e^{-k}\{Q_2(\omega + 2ik^2) + 1\},$$

$$\check{A}_{23} = -Q_3^{-1}e^{-k}\{Q_3(2i\hat{\eta}_3k^2 + \hat{\rho}_3\omega) + 1\}, \quad \check{\xi}_1 = 1 - \hat{\rho}_1 + k^2W_1, \quad \check{\xi}_2 = -1 + \hat{\rho}_3 + k^2W_2.$$

A non-trivial solutions of the unknown coefficients  $A_{pj}$ ,  $B_{lj}$ ,  $\hat{\xi}_l$ , of the system (27) exists if and only if the determinant of the  $14 \times 14$  matrix  $\mathbf{A}$  must be equal to zero, which yields a dispersion relation between the wavenumber  $k$  and the perturbation frequency  $\omega$  for specified values of other parameters, given by

$$F(\omega, k; R_e, E_{01}, \hat{\eta}_j, Q_j, W_l, \hat{\rho}_j, \hat{\varepsilon}_j) = 0, \quad (28)$$

which represents the linear dispersion equation for surface waves propagating through a viscous layer embedded between two other fluids with the influence of constant horizontal electric field. This dispersion relation controls the stability in the present problem. That is, each negative of the real part of  $\omega$  corresponds to a stable mode of the interfacial disturbance. On the other hand, if the real part of  $\omega$  is positive, the disturbance will grow in time and the flow becomes unstable.

It is clear that the eigenvalue relation (28) is somewhat more general and quite complex, since  $\ell_j$  involves square roots and so one can obtain other characteristic relation as limiting cases. For an inviscid fluid, we get the characteristic equation as a special case from Eq. (28) when  $\eta_j = 0$ . Thus by collecting the real and the imaginary terms in power order of  $\omega$  with the help of symbolic computation software *Mathematica*, Eq. (28) can be transformed into a polynomial algebraic equation of fourth order in the frequency  $\omega$ . Zakaria *et al.* [6] obtained a similar equation in their study of the temporal stability of inviscid fluids in porous media. Also, in the special case when the effect of the electric forces is absent and for the fluids flow through no-porous media, we get  $\ell_j = \sqrt{k^2 + \frac{\hat{\rho}_j R_e \omega}{\hat{\eta}_j}}$  and in this case, the dispersion relation (28) is reduced to a non-polynomial algebraic equation for the frequency  $\omega$  which coincides with that obtained by Kwak and Pozrikidis [17]. Another case is the limiting case of one interface between two continuum layers ( non-porous medium), in which highly viscous fluids are considered. Thus we obtain a polynomial equation of fifth order in  $\omega$ , which is obtained before by Kumar and Singh [14] and Sunil *et al.* [18].

In the following, numerical applications are carried out to demonstrate the effects of various physical parameters on the stability criteria of the system. In the present work, we will numerically solve the implicit dispersion relation

by means of the Chebyshev spectral tau method [19].

### 3.2 Numerical results

In order to discuss the stability diagrams, Eq. (28) is used to control the stability behavior, which requires specification of the parameters: the electric field, the dielectric constant, the porosity effect, the density, the viscosity. In the calculations given below all the physical parameters are sought in the dimensionless form as defined above. The stability of fluid sheets corresponds to negative values of the disturbance growth rate (i.e.  $\omega_r < 0$ ), and the disturbance growth rates of different fluids can be gained by solving the above corresponding dispersion relation numerically.

To screen the examinations of the electric field  $E_{01}$  on the stability criteria, numerical calculations for the dispersion relation (28) are made. The results for calculations are displayed in Fig. 2 in the plane  $(\omega_r - k)$ . The graph displayed in this plane is evaluated for a system having the parameters given in the caption of Fig. 2. Before, we discuss the stability of this graph we firstly define the critical wave number (also called the cutoff wave number) as given in [9] the value of the wave number at the point where the growth rate curve crosses the wave number axis in the plots of wave growth rate versus wave number. In other words the critical wave number is the value of the wave number, which separates the stable motions from the unstable ones and conversely, and can be obtained from the corresponding dispersion relations by setting  $\omega_r = 0$ . Since the stability arises according to the negative sign of the real part of the complex frequency  $\omega$ . Thus when the wave number is over the cutoff wave number, the fluid sheet is stable. In this figure the solid curve is plotted at the value  $E_{01} = 0.5$ , and the value  $E_{01} = 1$  corresponds to the dashed line, while the dotted curve represents the value  $E_{01} = 1.5$ . The inspection of Fig. 2 indicates that as the electric field is increased both the growth rates and the cutoff wave numbers reduced, on other meaning the unstable regions under the curves are decreased. Therefore, it is concluded that the electric field effects has a stabilizing influence in the fluid sheets.

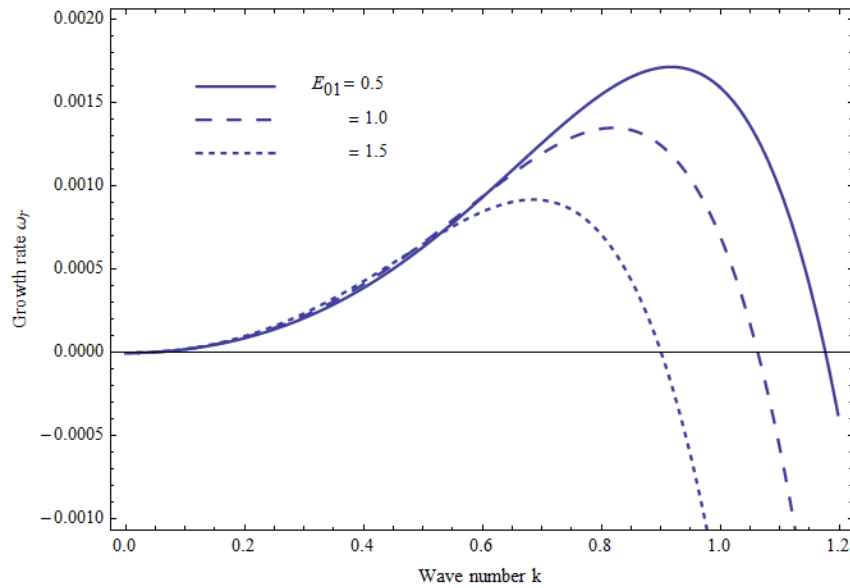


Figure 2: Effects of the electric field  $E_{01}$  in the plane  $(\omega_r - k)$  at  $\hat{\epsilon}_1 = 1.2$ ,  $\hat{\epsilon}_3 = 1.5$ ,  $\hat{\rho}_1 = 5$ ,  $\hat{\rho}_3 = 2$ ,  $R_e = 0.4$ ,  $\hat{\eta}_1 = 0.2$ ,  $\hat{\eta}_3 = 0.4$ ,  $Q_1 = 0.1$ ,  $Q_2 = 0.2$ ,  $Q_3 = 0.3$ ,  $W_1 = 2$ ,  $W_2 = 1$  on the wave growth rate, with  $E_{01}=0.5$  (solid), 1 (dashed), 1.5 (dotted).

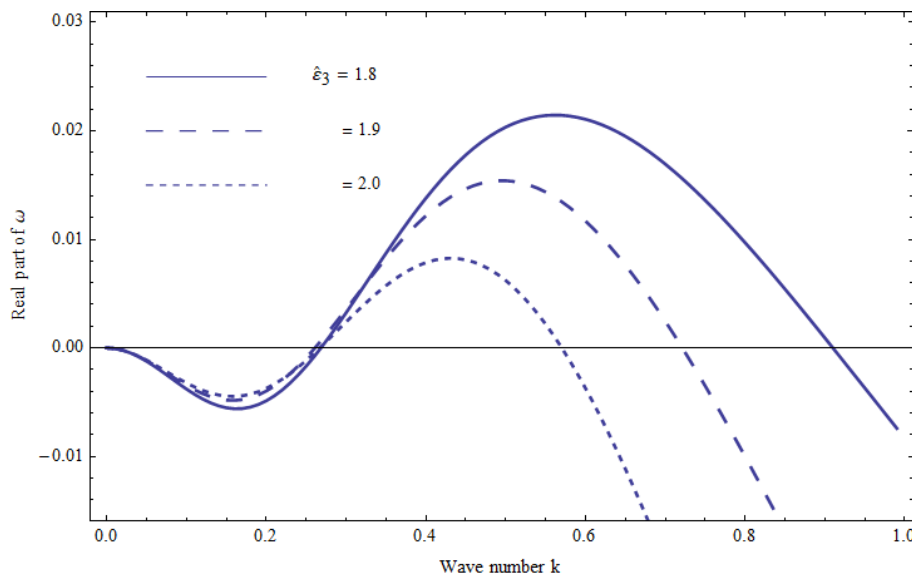


Figure 3: Influence of the dielectric parameter  $\hat{\epsilon}_3$  in the plane  $(\omega_r - k)$ , on the wave growth rate with  $\hat{\epsilon}_3=1.8, 1.9, 2$  at the same system given in Fig. 2.

The influence of changes of the dielectric constant ratio  $\hat{\epsilon}_3 (= \epsilon_3/\epsilon_2)$ , on the stability behavior in the plane  $(\omega_r - k)$  is illustrated in Fig. 3. The calcu-

lations are made for a system having the same parameters given in Fig. 2, while the dielectric ratio  $\hat{\epsilon}_3$  has some variation for the sake of comparison. In the graph 3 the values 1.8, 1.99 and 2 are selected for  $\hat{\epsilon}_3$  correspond to the continuous, dashed and dotted curves respectively. It is apparent from the inspection of Fig. 3, under the influence of the dielectric parameter  $\hat{\epsilon}_3$ , the growth rates with different dielectric constant ratio keep almost identical for the wave numbers less than 0.24, but increase correspondingly at higher values of the wave number, further the plane  $(\omega_r - k)$  is divided into two regions. The first is  $0 < k < 0.24$ , which represents a stabilizing effect for increasing the parameter  $\hat{\epsilon}_3$ . The second region lie in the range  $0.24 < k < 1$ , since in this range, we notice that, when the dielectric constant is increased, both the growth rates and the cutoff wave numbers of fluid sheets decrease. A general conclusion of the graph 3 reveals that the phenomenon of the dual (irregular) role is found for increasing the dielectric constant ratio  $\hat{\epsilon}_3$ , which there are two roles one is a stabilizing influence in the range  $k < 0.24$ , and the other is a destabilizing in the range  $0.24 < k < 1$ .

The examination of change of the lower to the middle fluid density ratio  $\hat{\rho}_1$  in the stability criteria is illustrated in Fig. 4.

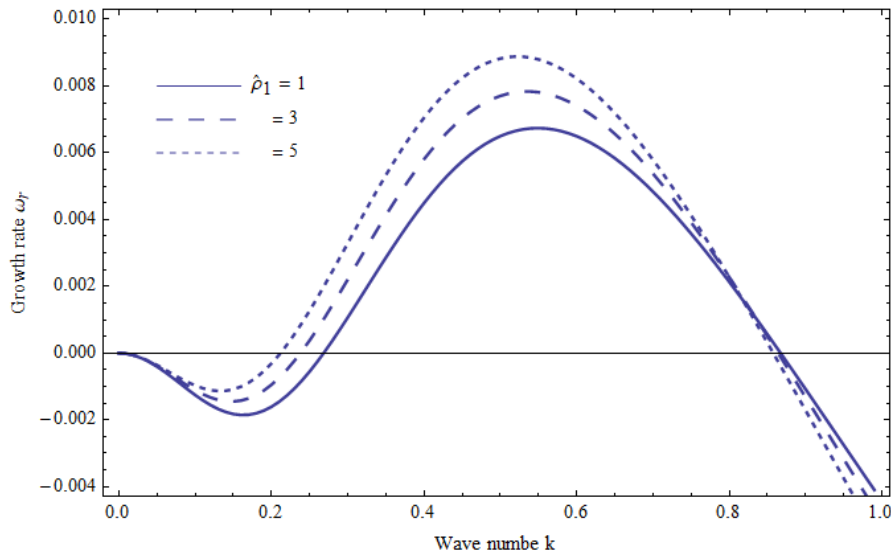


Figure 4: The graph is constructed for  $\omega_r$  versus  $k$ , with  $\hat{\rho}_1=1, 2, 3$ .

The graphs are constructed for  $\omega_r$  versus  $k$ , are achieved for three values of the ratio  $\hat{\rho}_1 = 1, 3$  and  $5$ , correspond to the continuous, dashed and dotted lines respectively, where the other quantities are held fixed. In this figure, the areas lie under  $k$ -axis and above the curves are stable and may be called stability

regions (corresponding to the negative values of  $\omega_r$ ), while the areas above the horizontal axis are unstable. The inspection of the stability diagram of Fig. 4 reveals that the increase of the density ratio  $\hat{\rho}_1$  leads to increase in the width of unstable regions. The result that may be made here is that the ratio  $\hat{\rho}_1$  has a destabilizing influence on the stability behavior of the waves. This result confirmed the fact that when the lower fluid is more heavier than the upper, thus the system is stable.

Fig. 5 exhibits the effects of the permeability parameter  $Q_1$  on the stability behavior of the fluid layers.

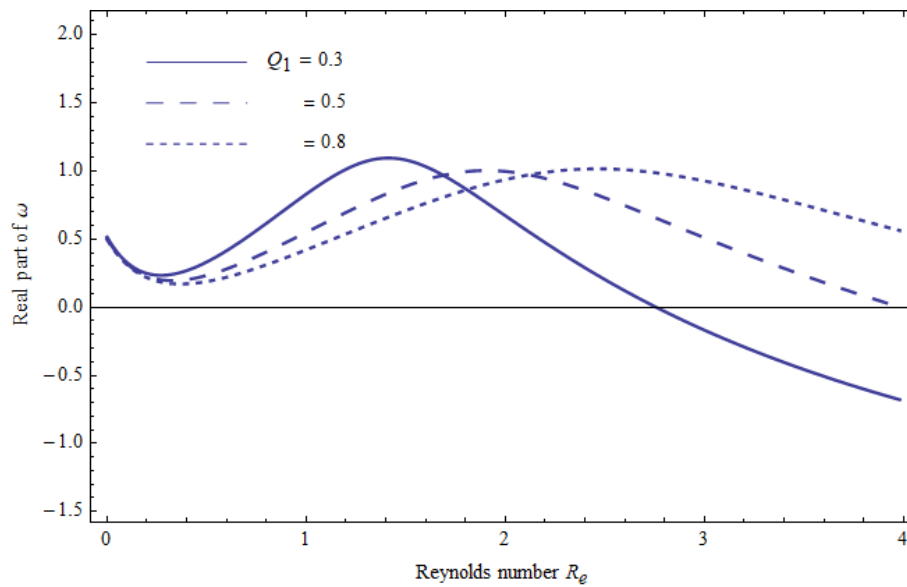


Figure 5: Illustrated in the plane  $(\omega_r - R_e)$  with the permeability parameter  $Q_1=0.3, 0.5, 0.8$ .

In this graph the solid, dashed and dotted curves represent the values 0.3, 0.5 and 0.8 in the plane  $(\omega_r - R_e)$  of the parameter  $Q_1$  respectively. Having noted the stability chart of this diagram, it is observed that the increase of the permeability in the range  $0 < R_e < 1.8$ , leads to a contraction in the width of the instability regions (the regions under the curves and above the wave number axis correspond to the positive sign of the disturbance growth rate). On the other hand, through the interval  $1.8 < R_e < 4$  the growth rates of instabilities with different  $Q_1$  are increased. In general view of the graph 5, it is noticed that there are two roles of the variation of the porous parameter  $Q_1$ , the first one is a stabilizing when the Reynolds number  $R_e$  less than the value 1.8, and the other role is a destabilizing when  $R_e$  lies between the values 1.8 and 4. Hence the phenomenon of the dual role is found for increasing the

permeability parameter  $Q_1$ .

The examination of change of the upper to the middle fluid viscosity ratio  $\hat{\eta}_3$  in the stability criteria is illustrated in Fig. 6, where the values 0.1, 0.2 and 0.3 are choosing for the quantity  $\hat{\eta}_3$ .

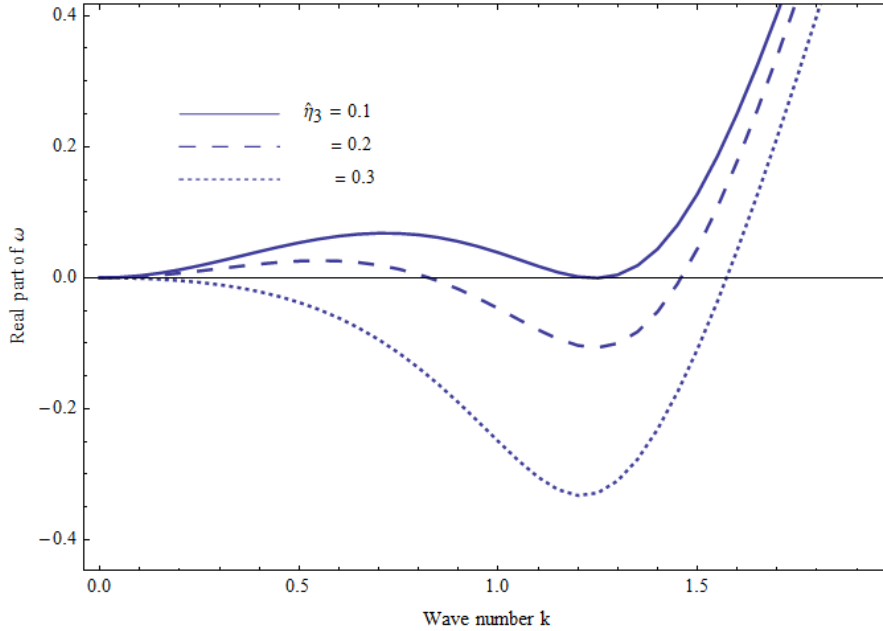


Figure 6: Represents the stability diagrams in the plane  $(\omega_r - k)$  at the viscosity ratio  $\hat{\eta}_3=0.1$  (solid), 0.2 (dashed), 0.3 (dotted).

It is obvious from this graph, for every value of the  $\hat{\eta}_3$ , the corresponding curve crosses the wave number axis at three points (the cutoff wave numbers) and formed areas of stability and instability regions. Inspection of Fig. 6 reveals that the increase of the viscosity ratio  $\hat{\eta}_3$  tends to a reduction in the width of the unstable regions, whereas the stability region extended under the influence of the increasing  $\hat{\eta}_3$ . It is clear that from Fig. 6 the viscosity ratio  $\hat{\eta}_3$  has a stabilizing influence on the stability of the movement of the waves. Ozen *et al.* [20] have been obtained a similar conclusion in their studies of electrohydrodynamic linear stability of two immiscible fluids in channel flow. In Fig. 7, in which the real part of the frequency  $\omega$  is plotted against the wave number, the Reynolds number  $R_e$  is varied stepwise from 0.2 to 0.6 to show its effect on the stability picture. Having checked the stability diagrams of this figure, it is discovered that the increase of the Reynolds number leads to an extension in the instability areas above the wave number axis, and consequently, the Reynolds number has a destabilizing role on the stability behavior. Similar results were

reported by Liu *et al.* [9] in their studies of the instability of two-dimensional non-Newtonian liquid sheets.

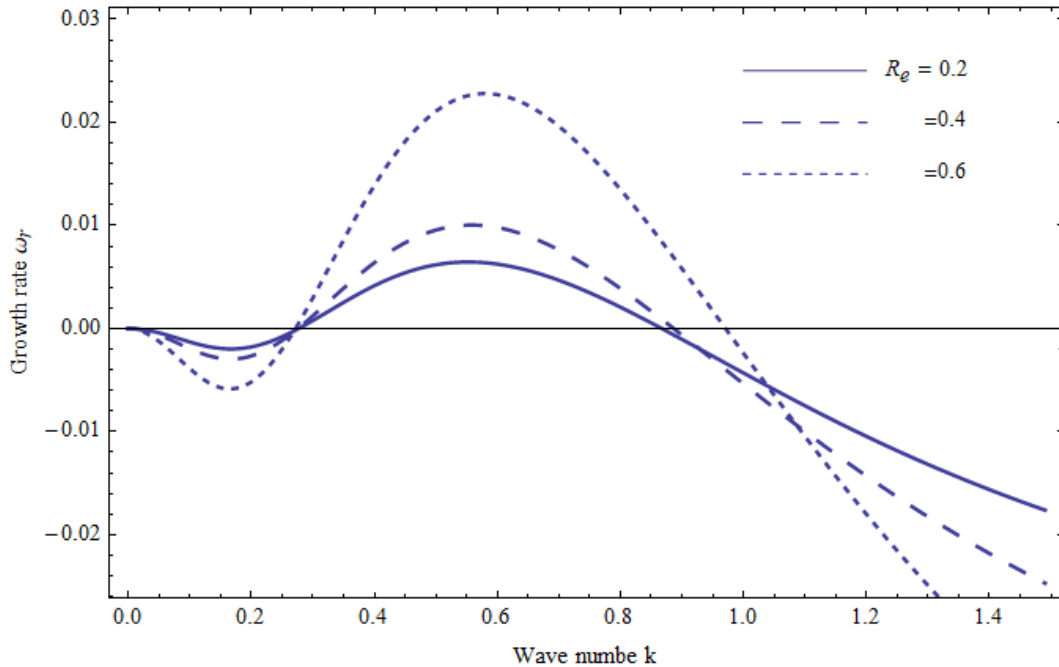


Figure 7: The graph is constructed for non-dimensional growth rate of different fluids versus non-dimensional wave number at Reynolds number  $R_e = 0.2, 0.4$  and  $0.6$ .

The influence of electric field  $E_{01}$  on the flow behavior in terms of streamlines field is illustrated through the parts of Fig. 8 (a curve formed by the velocity vectors of each fluid particle at a certain time is called a streamline, in which the tangent at each point of this curve indicates the direction of fluid at that point). The streamlines (curvilinear) in the physical domain are thus mapped into horizontal grid lines in the computational plane, thus resulting in a rectangular computational region. The streamlines show to be very effective tools to visualize a qualitative impression of the flow behavior during the motion. In the parts (a-c) of Fig. 8, the streamlines picture is achieved by fixing the value of all the physical parameters as given in Fig. 2, with  $k = 0.5$ ,  $t = 0.2$ ,  $\hat{\xi}_1 = 0.02$  and  $\hat{\xi}_2 = 0.06$  where  $E_{01}$  has three value for comparison. Snapshots of instantaneous streamlines of the stream function are shown in Fig.8(a) at  $E_{01}=0.5$ . The inspection of this graph reveals that the flow consists of cells (contours) consisting of clockwise ( positive values of streamlines) and anti-clockwise ( negative values of streamlines) circulations. In parts (b) and (c) of

this graph, the values of  $E_{01}$  are increased to 1 and 1.5 respectively.

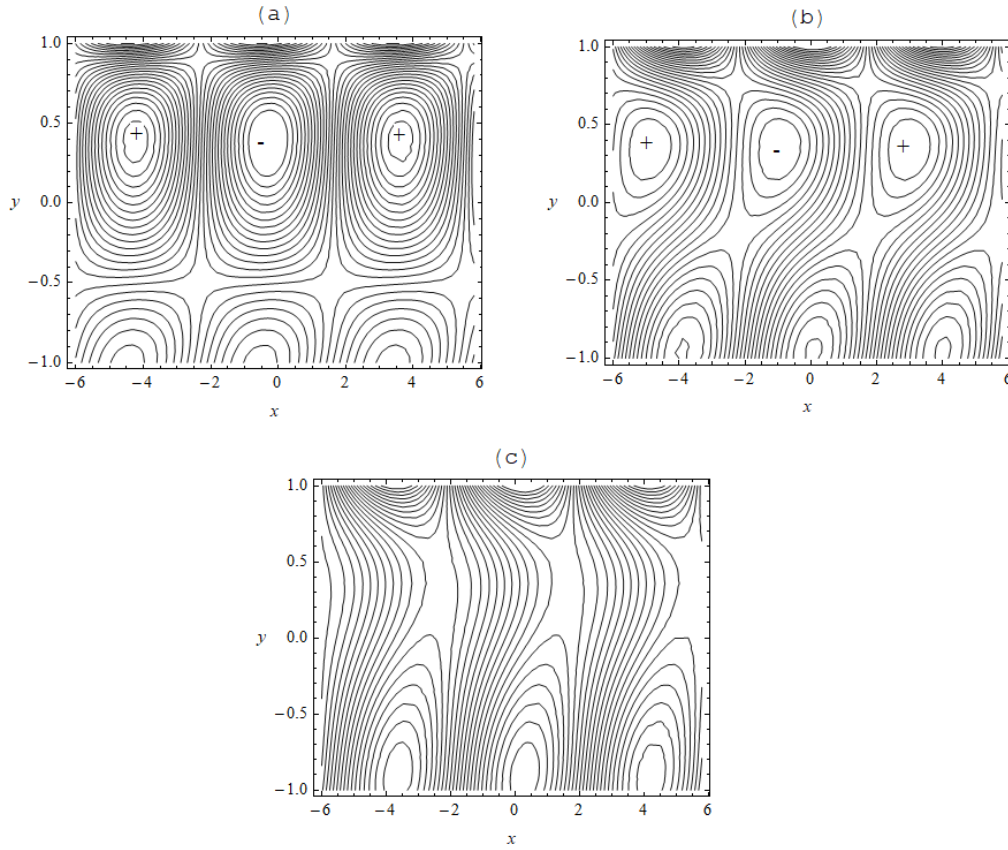


Figure 8: Streamlines contours for a system having the same parameters considered in Fig. 2, with  $k = 0.5$ ,  $t = 0.2$ ,  $\hat{\xi}_1 = 0.02$  and  $\hat{\xi}_2 = 0.06$ , where  $E_{01} = 0.5, 1$  and  $1.5$  of the parts (a), (b), (c) and (d), respectively.

A conclusion that may be made from the comparison among the parts (a-c) of Fig. 8 is that the electric field leads to a crowd in the concentration of the streamlines in the movement of the fluids. In other words, in the light of stability configuration, we notice that corresponding the parts (a-c) of Fig. 8 there are three different values of the disturbance growth rate ( $\omega_r$ ), which are  $-0.024$ ,  $-0.142$  and  $-0.603$ . Since the stability of fluid sheets arises to negative values of growth rate, thus it can be observed that the streamlines contours represent a stable system. Hence the electric field has stability influence, which coincides with the result given in Fig. 2.

## 4 Conclusions

In the present study, we have discussed the stability properties of two-dimensional viscous fluid layers moving in porous media, under the influence of an electric field. The solutions of the linearized equations of motion under the boundary conditions lead to an implicit dispersion relation between the growth rate and wave number. The parameters governing the layers flow system, the electric properties and porosity effects strongly influence the wave forms and their amplitudes and hence the stability of the fluid. The stability criteria have been performed theoretically and numerically in which the physical parameters are put in the dimensionless form. Some stability diagrams have been plotted and discussed, in which the influence of the various parameters of the problem on the interface stability is thoroughly analyzed.

It is established that the phenomenon of the dual (to be either stabilizing or destabilizing) role is found for increasing the permeability parameter as well as the dielectric ratio. It has been found that both the viscosity coefficient and the electric field damps the growth rate, introducing stabilizing influence, where a part of its kinetic energy may be absorbed. However, it is expected to be a more careful search would clarify that the motion of the interfacial waves will be more stable with the increase of the values of the viscosity as well as the electric field. An increase of the lower to the middle fluid density ratio enhances both the growth rate and the instability range of fluid sheet, which give a destabilizing influence on the stability behavior of the waves. This result confirmed the fact that when the lower fluid is more heavier than the upper, thus the system is stable. The role of Reynolds number and the density ratio is to increase the amplitude of the disturbance leading to the destabilization state of the flow system, promote the oscillatory behavior.

**Acknowledgements.** This work was supported and funded by "The Research Program of Public Authority for Applied Education and Training in Kuwait", project No (TS-17-02).

## References

- [1] P.K. Bhatia, Rayleigh-Taylor instability of two viscous superposed conducting fluids, *Nuovo Cimento*, **19B** (1974), 161-168.

- [2] T. Funada and D.D. Joseph, Viscous potential flow analysis of Kelvin-Helmholtz instability in a channel, *J. Fluid Mech.*, **445** (2001), 263-283. <https://doi.org/10.1017/s0022112001005572>
- [3] A.F. Elhefnawy, Intervals of an unsteady electrohydrodynamic Kelvin-Helmoltz stability, *Physica A: Statistical Mechanics and its Applications*, **214** (1995), 229-241. [https://doi.org/10.1016/0378-4371\(94\)00232-i](https://doi.org/10.1016/0378-4371(94)00232-i)
- [4] P.G. Drazin and W.H. Reid, *Hydrodynamic Stability*, Univ. Press, Cambridge, 1981.
- [5] D.D. Joseph, *Stability of Fluid Motions II*, Springer-Verlag, New York, 1976. <https://doi.org/10.1007/978-3-642-80994-1>
- [6] K. Zakaria, M.A. Sirwah and S. Alkharashi, Temporal stability of superposed magnetic fluids in porous media, *Physica Scripta*, **77** (2008), 1-20. <https://doi.org/10.1088/0031-8949/77/02/025401>
- [7] K. Zakaria, M. A. Sirwah, S. A. Alkharashi, Non-linear analysis of creeping flow on the inclined permeable substrate plane subjected to an electric field, *Int. J. of Non-Linear Mech.*, **47** (2012), 577-598. <https://doi.org/10.1016/j.ijnonlinmec.2011.11.010>
- [8] A.W. Wray, D.T. Papageorgiou and O.K. Matar, Electrified coating flows on vertical fibres: enhancement or suppression of interfacial dynamics, *J. Fluid Mech.*, **735** (2013), 427-456. <https://doi.org/10.1017/jfm.2013.505>
- [9] Z. Liu, G. Brenn, F. Durst, Linear analysis of the instability of two-dimensional non-Newtonian liquid sheets, *J. Non-Newtonian Fluid Mech.*, **78** (1998), 133-166. [https://doi.org/10.1016/s0377-0257\(98\)00060-3](https://doi.org/10.1016/s0377-0257(98)00060-3)
- [10] M.A. Sirwah, Linear instability of the electrified free interface between two cylindrical shells of viscoelastic fluids through porous media, *Acta Mech. Sinica*, **28** (2012), no. 6, 1572-1589. <https://doi.org/10.1007/s10409-012-0208-2>
- [11] W.C. Tan and T. Masuoka, Stokes' first problem for an Oldroyd-B fluid in a porous half space, *Phys. Fluids*, **17** (2005), 023101. <https://doi.org/10.1063/1.1850409>

- [12] K. Zakaria, Long interfacial waves inside an inclined permeable channel, *Int. J. of Non-Linear Mech.*, **47** (2012) 42-48.  
<https://doi.org/10.1016/j.ijnonlinmec.2012.02.002>
- [13] M. Khan, M. Saleem, C. Fetecau and T. Hayat, Transient oscillatory and constantly accelerated non-Newtonian flow in a porous medium, *Int. J. of Non-Linear Mech.*, **42** (2007), 1224-1239.  
<https://doi.org/10.1016/j.ijnonlinmec.2007.09.008>
- [14] P. Kumar and G.J. Singh, Stability of two superposed Rivlin-Ericksen viscoelastic fluids in the presence of suspended particles, *Rom. J. Phys.*, **51** (2006), 927-935.
- [15] H.H. Woodson and J.R. Melcher, *Electromechanical Dynamics*, John Wiley, Sons., 1968.
- [16] R.E. Rosensweig, *Ferrohydrodynamics*, Cambridge: Cambridge University Press, 1985.
- [17] S. Kwak, C. Pozrikidis, Effect of surfactants on the instability of a liquid thread of annular layer. Part I: Quiescent fluids, *Int. J. Multiphase Flow*, **27** (2001), 1-37. [https://doi.org/10.1016/s0301-9322\(00\)00011-2](https://doi.org/10.1016/s0301-9322(00)00011-2)
- [18] Sunil, R.C. Sharma and R.S. Chandel, On superposed couple-stress fluids in porous medium in hydromagnetics the Use of Quantum-Chemical Semiempirical Methods to Calculate the Lattice Energies of Organic Molecular Crystals. Part II: The Lattice Energies of - and -Oxalic Acid (COOH)<sub>2</sub>, *Z. Naturforsch. A*, **57a** (2002), 955-960.  
<https://doi.org/10.1515/zna-2002-1208>
- [19] J.P. Boyd, *Chebyshev and Fourier Spectral Methods*, Dover Publications. Inc., Mineola, NY 2001.
- [20] O. Ozen, N. Aubry, D.T. Papageorgiou and P.G. Petropoulos, Electrohydrodynamic linear stability of two immiscible fluids in channel flow, *Electrochimica Acta*, **51** (2006), 5316-5323.  
<https://doi.org/10.1016/j.electacta.2006.02.002>

**Received: June 5, 2018; Published: June 28, 2018**